# NACA

# RESEARCH MEMORANDUM

AERODYNAMIC CHARACTERISTICS OF A WING WITH QUARTER-CHORD

LINE SWEPT BACK 60°, ASPECT RATIO 4, TAPER

RATIO 0.6, AND NACA 65A006 AIRFOIL SECTION

TRANSONIC-BUMP METHOD

By Thomas J. King, Jr., and Boyd C. Myers, II

Langley Aeronautical Laboratory
Langley Air Force Base, Va.

CLASSIFIED DOCUMENT

This document contains classified information affecting the National Defense of the United States within the meaning of the Espionage Act, USC 50:31 and 32. Its transmission or the revelation of its contents in any manner to an unauthorized person is prohibited by law. Information so classified may be imparted only to persons in the military and naval services of the United States, appropriate civilian officers and employees of the Federal Government who have a legitimate interest therein, and to United States citizens of known loyalty and discretion who of necessity must be informed thereof.

CLASSIFICATION CHANGED TO
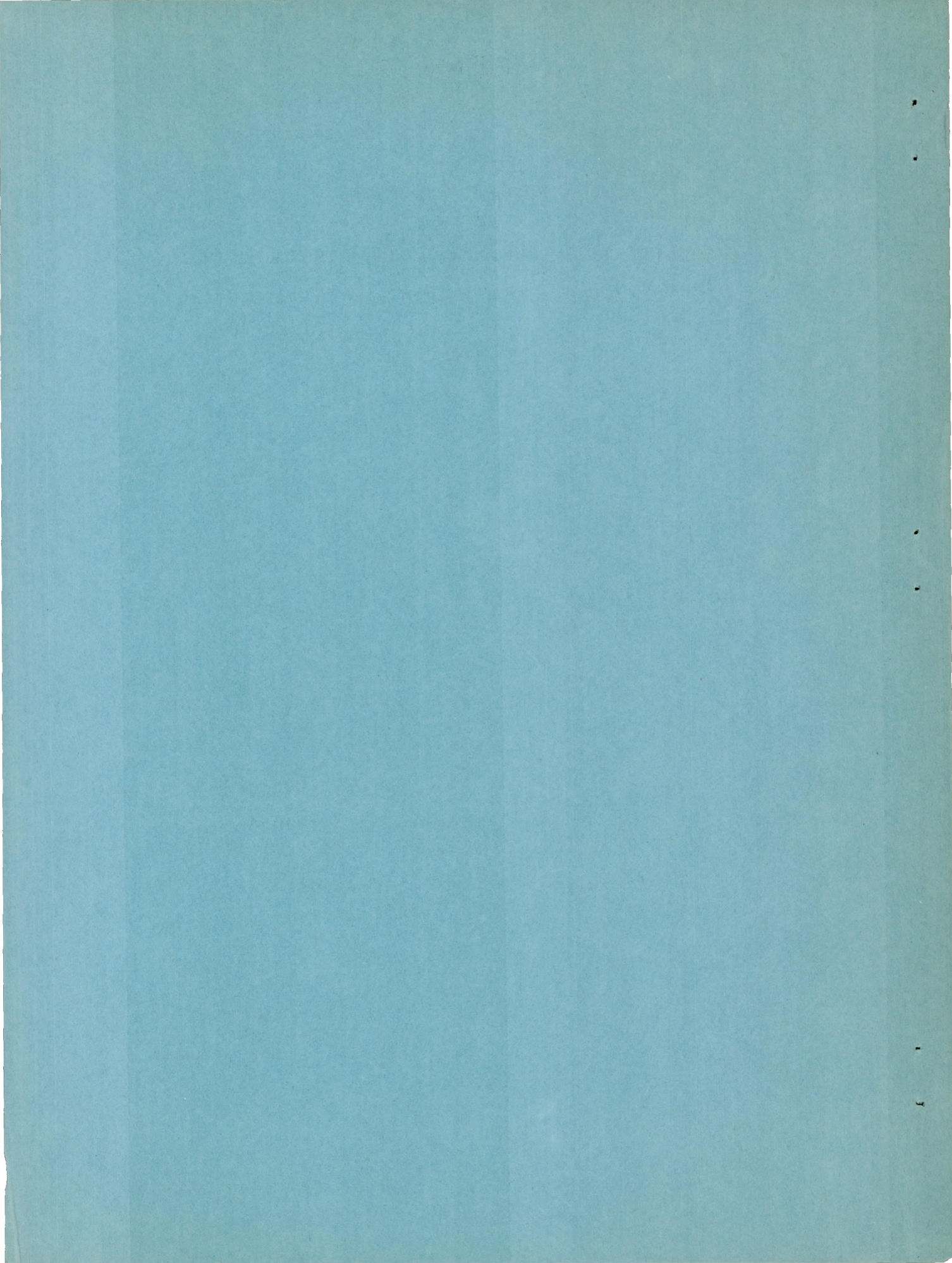UNCLASSIFIED
DATE 8-18-
AUTHORITY J.W.CROWLEY
CHANGE # 2453
W.H.L.

# NATIONAL ADVISORY COMMITTEE
# FOR AERONAUTICS

WASHINGTON
September 6, 1949

CONFIDENTIAL

## NATIONAL ADVISORY COMMITTEE FOR AERONAUTICS

## RESEARCH MEMORANDUM

AERODYNAMIC CHARACTERISTICS OF A WING WITH QUARTER-CHORD

LINE SWEPT BACK 60°, ASPECT RATIO 4, TAPER

RATIO 0.6, AND NACA 65A006 AIRFOIL SECTION

TRANSONIC-BUMP METHOD

By Thomas J. King, Jr., and Boyd C. Myers, II

## SUMMARY

As part of a transonic research program, a series of wing-body combinations are being investigated in the Langley high-speed 7- by 10-foot tunnel over a Mach number range from about 0.60 to 1.18, by use of the transonic-bump test technique.

This paper presents the results of the investigation of a wing-alone and a wing-fuselage configuration employing a wing with quarter-chord line swept back 60°, aspect ratio 4, taper ratio 0.6, and an NACA 65A006 airfoil section. The results are presented as lift, drag, pitching-moment, and bending-moment coefficients for both configurations. The effect of a wing fence on the wing-fuselage characteristics was also investigated. In addition, effective downwash angles and point dynamic pressures for a range of tail heights at a probable tail length are presented for the two configurations investigated. Only a brief analysis is given in order to facilitate the publishing of the data.

## INTRODUCTION

A series of wing-fuselage combinations is being investigated in the Langley high-speed 7- by 10-foot tunnel to study the effects of wing geometry on longitudinal stability characteristics at transonic speeds. In the transonic-bump technique used, a Mach number range of 0.60 to 1.18 is obtained. Previous data published in this series are presented in references 1 to 3.

This paper presents the results of the investigation of the wing—
alone and wing—fuselage configurations employing a wing with the
quarter—chord line swept back 60°, aspect ratio 4, taper ratio 0.6, and
an NACA 65A006 airfoil section parallel to the free stream.

## MODEL AND APPARATUS

The wing of the semispan model had 60° of sweepback referred to the
quarter—chord line, aspect ratio 4, taper ratio 0.6, and an NACA 65A006
airfoil section (reference 4) parallel to the free stream. The wing was
made of steel and the fuselage of brass. A two—view drawing of the
model is presented in figure 1 and ordinates of the fuselage of fineness
ratio 10 are given in table I. Details of a wing—fence arrangement
tested are shown in figure 2.

The model was mounted on an electrical strain—gage balance enclosed
in the bump, and the lift, drag, pitching moment, and bending moment
about the model plane of symmetry were measured with calibrated
potentiometers.

Effective downwash angles were determined for a range of tail
heights by measuring the floating angles of the tails at five different
positions with calibrated slide—wire potentiometers. Details of the
floating tails are given in figures 2 and 3, while a view of the model
mounted on the bump, showing three of the floating tails, is given
in figure 4. The tails used in this investigation are the same as those
used in references 1 to 3.

A total—pressure rake was used to determine the dynamic—pressure
ratios for a range of tail heights in a plane which contained the
25—percent mean—aerodynamic—chord point of the free—floating tails. The
total—pressure tubes were spaced 1/8 inch apart near the chord line
extended and 1/4 inch apart elsewhere.

## COEFFICIENTS AND SYMBOLS

$C_L$     lift coefficient $\left(\dfrac{\text{Twice panel lift}}{qS}\right)$

$C_D$     drag coefficient $\left(\dfrac{\text{Twice panel drag}}{qS}\right)$

$C_m$     pitching-moment coefficient referred to $0.25\overline{c}$

$$\left(\frac{\text{Twice panel pitching moment}}{qS\overline{c}}\right)$$

$C_B$     bending-moment coefficient about root chord line (at plane of symmetry)

$$\left(\frac{\text{Root bending moment}}{q\,\frac{S}{2}\,\frac{b}{2}}\right)$$

$q$     effective dynamic pressure over span of model, pounds per square foot $\left(\rho V^2/2\right)$

$S$     twice wing area of semispan model, 0.125 square foot

$\overline{c}$     mean aerodynamic chord of wing, 0.181 foot; based on relationship $\dfrac{2}{S}\displaystyle\int_{0}^{b/2} c^2\,dy$ (using the theoretical tip)

$c$     local wing chord

$\overline{c}_t$     mean aerodynamic chord of tail

$b$     twice span of semispan model

$y$     spanwise distance from wing root

$\rho$     air density, slugs per cubic foot

$V$     free-stream velocity, feet per second

$M$     effective Mach number over span of model

$M_l$     local Mach number

$M_a$     average chordwise local Mach number

$R$     Reynolds number of wing based on $\overline{c}$

$\alpha$     angle of attack, degrees

$\epsilon$     effective downwash angle, degrees

$\dfrac{q_{wake}}{q}$     ratio of point dynamic pressure, along a line containing the quarter-chord points of the mean aerodynamic chords of the free-floating tails, to the local free-stream dynamic pressure

$h_t$        tail height relative to wing chord plane extended, percent
             semispan; positive for tail positions above chord plane
             extended

a.c.         aerodynamic center

Subscripts:

M            at constant Mach number

$C_L = 0$    at zero lift


## TESTS


The tests were conducted in the Langley high-speed 7- by 10-foot
tunnel by use of an adaptation of the NACA wing-flow technique for
obtaining transonic speeds. The method used involves the mounting of
a model in the high-velocity flow field generated over the curved
surface of a bump located on the tunnel floor. (See reference 5.)

Typical contours of local Mach numbers in the region of the model
location on the bump, obtained from surveys with no model in position,
are shown in figure 5. There is a Mach number gradient which results
in a difference of about 0.04 over the span of the model at the lowest
and highest Mach numbers with a maximum difference of about 0.07 present
at a Mach number of about 1.0. The chordwise Mach number variation is
generally less than 0.01. No attempt has been made to evaluate the
effects of these spanwise and chordwise variations in Mach number. The
long-dashed lines shown near the wing root represent a local Mach
number 5 percent below the maximum value and indicate the extent of the
bump boundary layer. The effective test Mach number was obtained from
contour charts similar to those presented in figure 5 from the
relationship

$$M = \frac{2}{S} \int_0^{b/2} c M_a \, dy$$

The variation of mean test Reynolds number with Mach number is
shown in figure 6. The boundaries in the figure indicate the range in
Reynolds number caused by variations in test conditions during the
course of the investigation.

Force and moment data, effective downwash angles, and the ratio of
dynamic pressure at 25 percent of the mean aerodynamic chords of the
free-floating tails to free-stream dynamic pressure were obtained for

the model configurations tested through a Mach number range of 0.60 to 1.18 and an angle-of-attack range of -2° to 8°.

The end-plate tares on drag were obtained through the test Mach number range at zero angle of attack by testing the model configurations without end plates. For these tests a gap of about 1/16 inch was maintained between the wing root and the bump surface, and a sponge-wiper seal was fastened to the wing butt beneath the surface of the bump to prevent leakage (fig. 4(b)). The drag end-plate tares were assumed to be invariant with angle of attack and the tares obtained at zero angle of attack were applied to all drag data. Jet-boundary corrections have not been evaluated inasmuch as the boundary conditions to be satisfied are not rigorously defined. However, inasmuch as the effective flow field is large compared with the span and chord of the model, these corrections are believed to be small.

The possibility of change in aerodynamic characteristics of the wing due to twist resulting from bending under aerodynamic loading was considered. From static loading tests and reference 6, it was estimated that at the highest Mach number attained the effect of twist would be to cause a forward aerodynamic-center movement of about 2 percent. No corrections have been applied to the data presented.

From measurements of tail floating angles without a model installed, it was determined that a tail spacing of 2 inches relative to the wing chord plane would produce negligible interference effects of reflected shock waves on the tail floating angles. Downwash angles for the wing-alone configuration were therefore obtained simultaneously for the middle, highest, and lowest tail positions in one series of tests and for the two intermediate positions in succeeding runs. (See fig. 3.) For the wing-fuselage tests the effective downwash angles at the chord plane extended were determined by mounting a free-floating tail on the center line of the fuselage. The downwash angles presented are increments from the tail floating angles without a model in position. It should be noted that the floating angles measured are actually a measure of the angle of zero pitching moment about the tail-pivot axis rather than of the angle of zero lift. It has been estimated that, for the tail arrangement used, a 2° spanwise downwash gradient over the tail will result in an error of less than 0.2° in the resultant floating angle.

Total pressures obtained from the tail survey rake have been corrected for bow-wave loss. The static-pressure values used in computing dynamic-pressure ratios were obtained by use of a static probe without a model in position.

## RESULTS AND DISCUSSION

A table of the figures presenting the results follows:

Unless noted, the discussion is based on the summary curves presented in figure 14. The slopes have been averaged at $C_L = 0$ over a lift-coefficient range of $\pm 0.1$.

### Lift and Drag Characteristics

The wing-alone lift-curve slope (fig. 14) was a constant value of 0.042 from a Mach number of 0.60 to 0.96. Unpublished low-speed data from the Langley two-dimensional low-turbulence tunnel for a geometrically similar model also gives a value of 0.042 (Reynolds number, $1.5 \times 10^6$). Above a Mach number of 0.96, the wing-alone lift-curve slope decreased to 0.038 at $M = 1.04$ and remained constant to a Mach number of 1.18. The addition of the fuselage increased the lift-curve slope approximately 10 percent throughout the test Mach number range.

At a Mach number of 0.60 (see fig. 14), the wing-alone minimum drag coefficient was about 0.006 as compared with an average minimum-drag-coefficient value of 0.0045 obtained at low speed in the Langley two-dimensional low-turbulence tunnel for a model of the same geometric characteristics (Reynolds number, $1.5 \times 10^6$ to $6.0 \times 10^6$). (Note that the drag coefficients presented have been corrected for end-plate tares while the drag data of references 1 to 3 have not been so corrected.) At zero lift, the wing-alone drag-rise Mach number is not readily apparent since the rate of increase in drag coefficient is quite low. It should be noted that the drag coefficient attained at the highest Mach number was only 0.012. For the wing-fuselage configuration the drag rise occurred at about $M = 1.02$ and the rate of drag rise was considerably more pronounced than for the wing-alone configuration. No correction for the fuselage base pressure has been applied to the wing-fuselage drag data.

## Pitching-Moment Characteristics

Near zero lift coefficient the wing-alone aerodynamic center was about 34 percent mean aerodynamic chord up to a Mach number of 0.97. Extrapolation and interpolation of data from reference 7 indicate a theoretical aerodynamic-center location of about 30 percent mean aerodynamic chord, although unpublished Langley two-dimensional low-turbulence-tunnel data on a geometrically similar wing gave an aerodynamic-center position of only 23 percent mean aerodynamic chord. The addition of the fuselage to the isolated wing moved the aerodynamic center rearward about 2 percent mean aerodynamic chord up to a Mach number of 0.90. Above $M = 0.90$, the rearward aerodynamic-center movement caused by the fuselage increased rapidly and was about 30 percent mean aerodynamic chord at $M = 1.15$. It can be seen in figures 7 and 8 that the pitching-moment curves indicate a trend toward instability at the relatively low lift coefficient of about 0.20 throughout the Mach number range.

## Effect of Wing Fence

In an attempt to alleviate the unstable trend of the pitching-moment curves at a relatively low lift coefficient, a wing fence (fig. 2) located on the mean aerodynamic chord was investigated on the wing-fuselage configuration. Near zero lift the fence appeared to decrease the slope of the pitching-moment curves slightly at the lowest and highest Mach numbers with a somewhat more inboard location of the lateral center of pressure indicated from the bending-moment curves. (See fig. 9.) At the highest lift coefficients obtained $\left(C_L \approx 0.3 \text{ to } 0.4\right)$ the fence produced a pronounced stabilizing trend in the pitching-moment characteristics at all Mach numbers and the lift-curve slope appeared to be increased somewhat.

## Downwash and Dynamic-Pressure Surveys in Region of Tail Plane

The downwash gradient $(\partial \epsilon/\partial \alpha)_M$ for the wing alone varied little with tail height through the Mach number range. (See fig. 12.) Near zero tail height the addition of the fuselage appreciably increased the downwash gradient $(\partial \epsilon/\partial \alpha)_M$ as the tail height approached the chord plane. At the higher lift coefficients, for both the wing-alone and wing-fuselage configurations, $(\partial \epsilon/\partial \alpha)_M$ would appear to be generally lower for tail heights below the chord plane and higher for tail heights above the chord plane through the Mach number range (figs. 10 and 11).

The results of point dynamic–pressure surveys, made in a plane
perpendicular to the chord plane extended at α = 0°, containing the
25 percent mean–aerodynamic–chord points of the free-floating tails used
in the downwash surveys, are presented in figure 13.  There is very
little change in the wake characteristics as the Mach number is increased
to 1.10.  The addition of the fuselage had little effect on the dynamic-
pressure ratios through the Mach number range.


Langley Aeronautical Laboratory
    National Advisory Committee for Aeronautics
        Langley Air Force Base, Va.



REFERENCES


1. Weil, Joseph, and Goodson, Kenneth W.:  Aerodynamic Characteristics
      of a Wing with Quarter–Chord Line Swept Back 45°, Aspect Ratio 4,
      Taper Ratio 0.6, and NACA 65A006 Airfoil Section.  Transonic–Bump
      Method.  NACA RM L9A21, 1949.

2. Sleeman, William C., Jr., and Becht, Robert E.:  Aerodynamic Charac-
      teristics of a Wing with Quarter–Chord Line Swept Back 35°, Aspect
      Ratio 4, Taper Ratio 0.6, and NACA 65A006 Airfoil Section.
      Transonic–Bump Method.  NACA RM L9B25, 1949.

3. Myers, Boyd C., II, and King, Thomas J., Jr.:  Aerodynamic Character-
      istics of a Wing with Quarter–Chord Line Swept Back 45°, Aspect
      Ratio 4, Taper Ratio 0.3, and NACA 65A006 Airfoil Section.
      Transonic–Bump Method.  NACA RM L9E25, 1949.

4. Loftin, Laurence K., Jr.:  Theoretical and Experimental Data for a
      Number of NACA 6A–Series Airfoil Sections.  NACA TN 1368, 1947.

5. Schneiter, Leslie E., and Ziff, Howard L.:  Preliminary Investigation
      of Spoiler Lateral Control on a 42° Sweptback Wing at Transonic
      Speeds.  NACA RM L7F19, 1947.

6. Stevens, Victor I.:  Theoretical Basic Span Loading Characteristics
      of Wings with Arbitrary Sweep, Aspect Ratio, and Taper Ratio.
      NACA TN 1772, 1948.

7. DeYoung, John:  Theoretical Additional Span Loading Characteristics
      of Wings with Arbitrary Sweep, Aspect Ratio, and Taper Ratio.
      NACA TN 1491, 1947.

## TABLE I.— FUSELAGE ORDINATES

[Basic fineness ratio 12; actual fineness ratio 10
achieved by cutting off the rear one-sixth of
the body; $\overline{c}/4$ located at $l/2$]
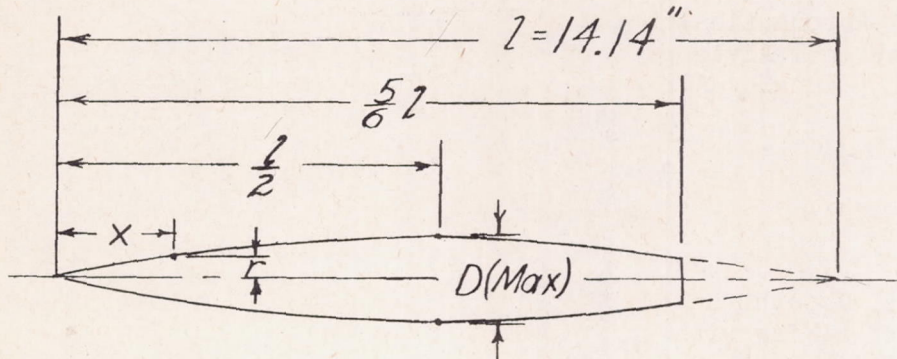


| Ordinates | | | | |
|---|---|---|---|---|
| $x/l$ | $r/l$ | | $x/l$ | $r/l$ |
| 0 | 0 | | 0 | 0 |
| .005 | .00231 | | .4500 | .04143 |
| .0075 | .00298 | | .5000 | .04167 |
| .0125 | .00428 | | .5500 | .04130 |
| .0250 | .00722 | | .6000 | .04024 |
| .0500 | .01205 | | .6500 | .03843 |
| .0750 | .01613 | | .7000 | .03562 |
| .1000 | .01971 | | .7500 | .03128 |
| .1500 | .02593 | | .8000 | .02526 |
| .2000 | .03090 | | .8338 | .02000 |
| .2500 | .03465 | | .8500 | .01852 |
| .3000 | .03741 | | .9000 | .01125 |
| .3500 | .03933 | | .9500 | .00439 |
| .4000 | .04063 | | 1.0000 | 0 |
| L. E. radius = 0.0005$l$ | | | | |
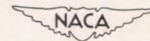
CONFIDENTIAL

Tabulated Wing Data

| | |
|---|---|
| Area (Twice semispan) | 0.125 sq ft |
| Mean aerodynamic chord | 0.1805 ft |
| Aspect ratio | 4.0 |
| Taper ratio | 0.6 |
| Incidence | 0.0° |
| Dihedral | 0.0° |
| Airfoil section parallel to free stream | NACA 65A006 |

1.591

60°

0.25-Chord line

2.166

4.243

1.944

90°

2.652

Reference centerline

Bump surface

Clearance 1/16

11.8

Centerline of balance
normal to bump surface
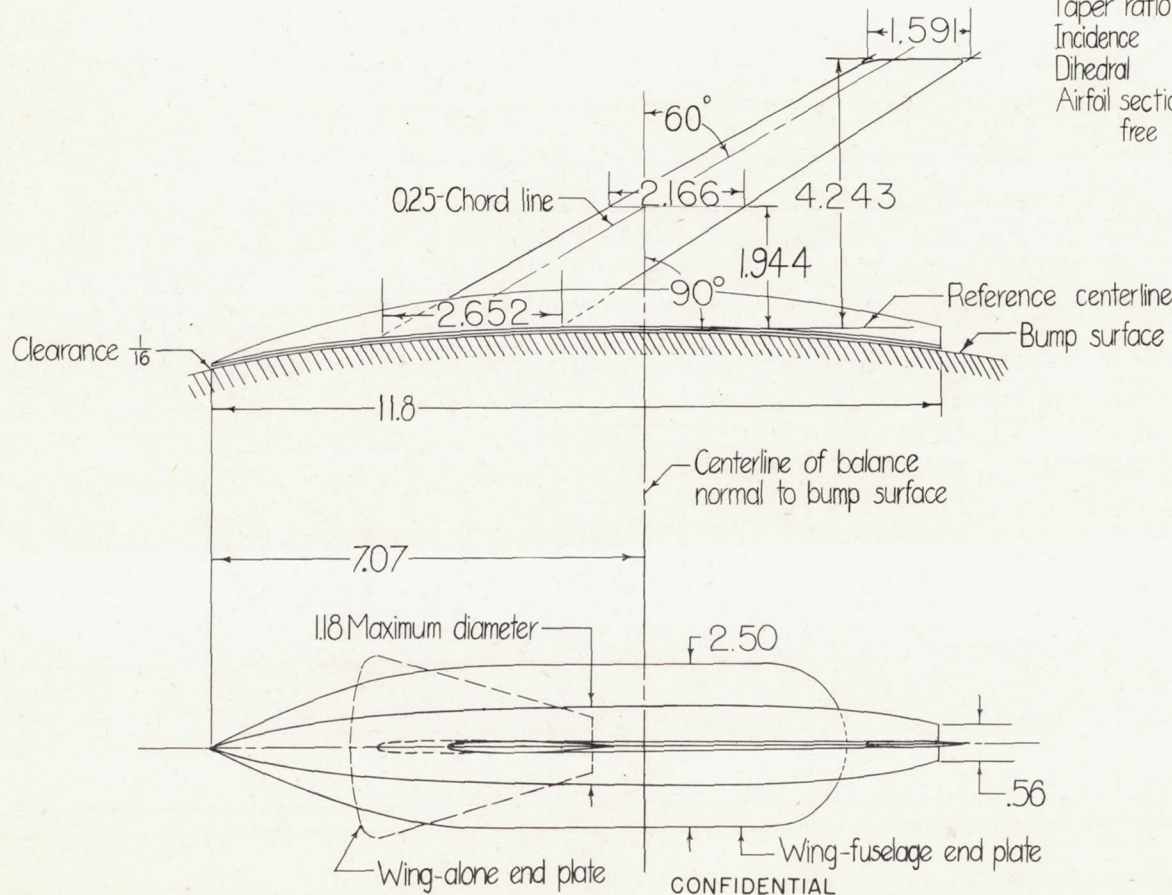
All dimensions
in inches

7.07

1.18 Maximum diameter

2.50

0   1   2
Scale,inches
NACA

.56

Wing-alone end plate

Wing-fuselage end plate
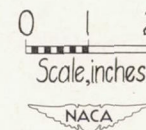
CONFIDENTIAL

Figure 1.- General arrangement of model with 60° sweptback wing, aspect ratio 4, taper ratio 0.6, and NACA 65A006 airfoil.
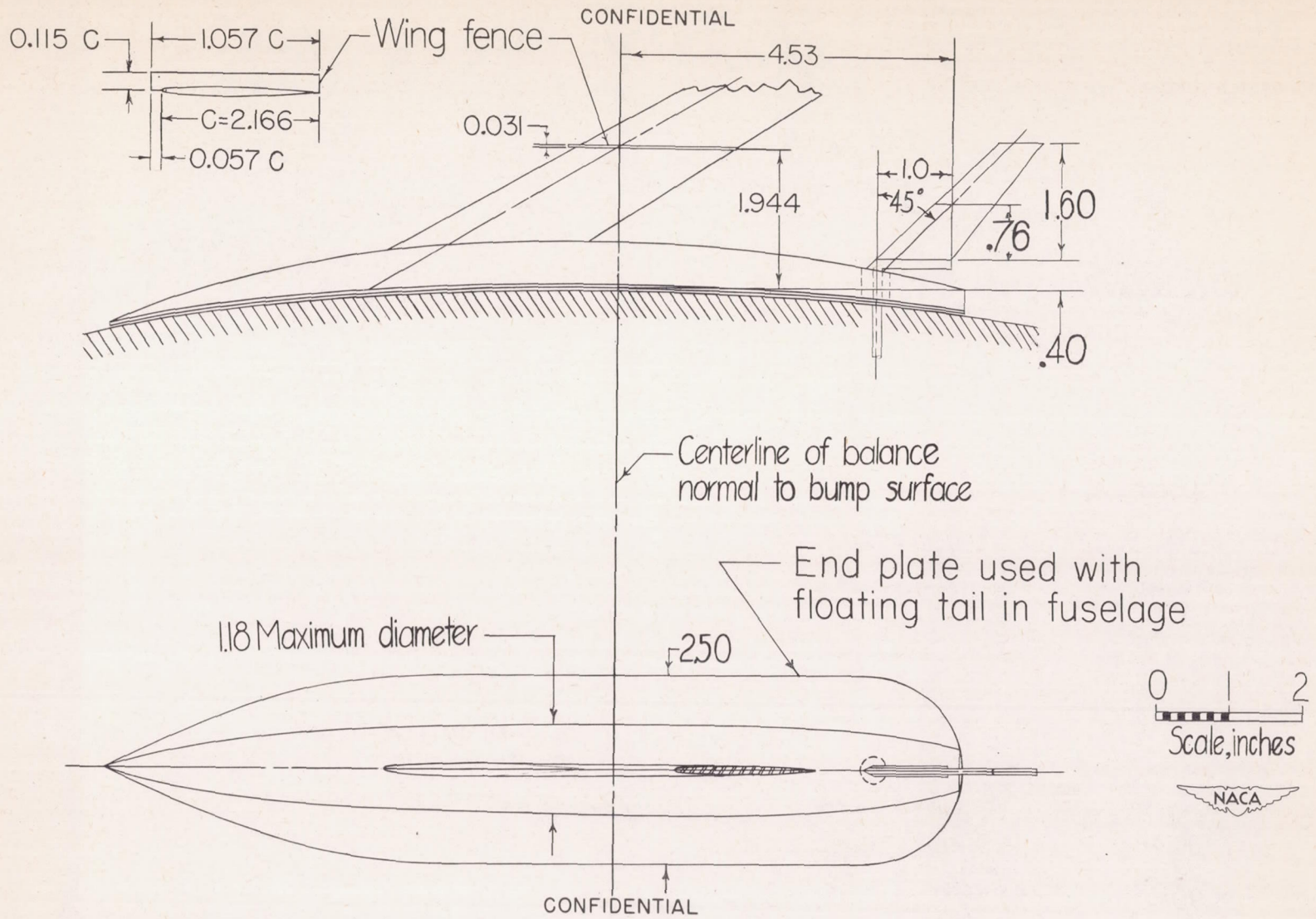
Figure 2.- Details of wing fence and free-floating tail mounted on a model with 60° sweptback wing, aspect ratio 4, taper ratio 0.6, and NACA 65A006 airfoil.

Floating-tail geometry

| | |
|---|---|
| Twice semispan area | 0.0178 sq ft |
| Aspect ratio | 4.0 |
| Taper ratio | 0.60 |

Chord plane
$\alpha = 0°$

Section B-B

Double scale

Scale , inches
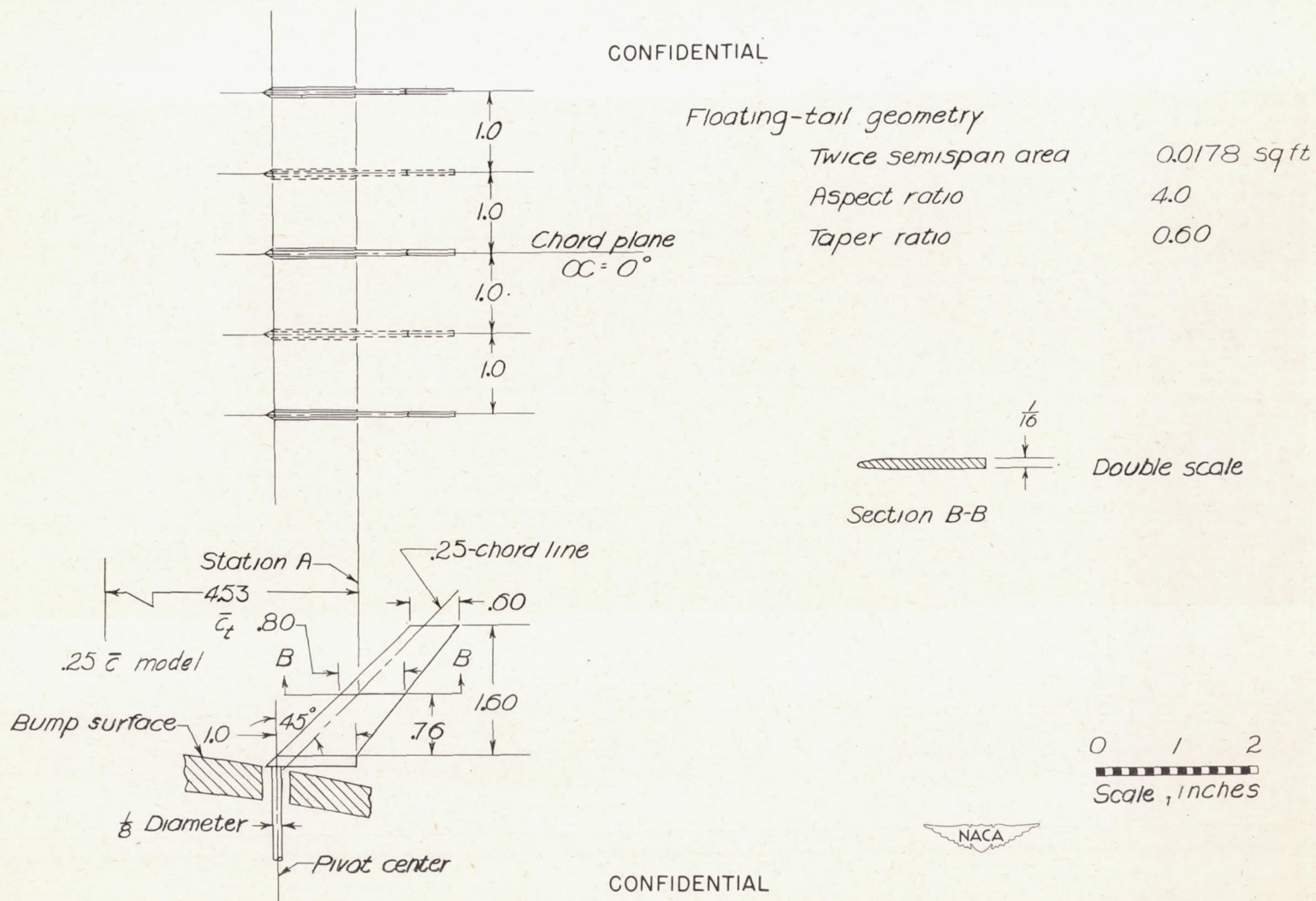
NACA

Figure 3.- Details of free-floating tails used in surveys behind model with $60°$ sweptback wing, aspect ratio 4, taper ratio 0.6, and NACA 65A006 airfoil.
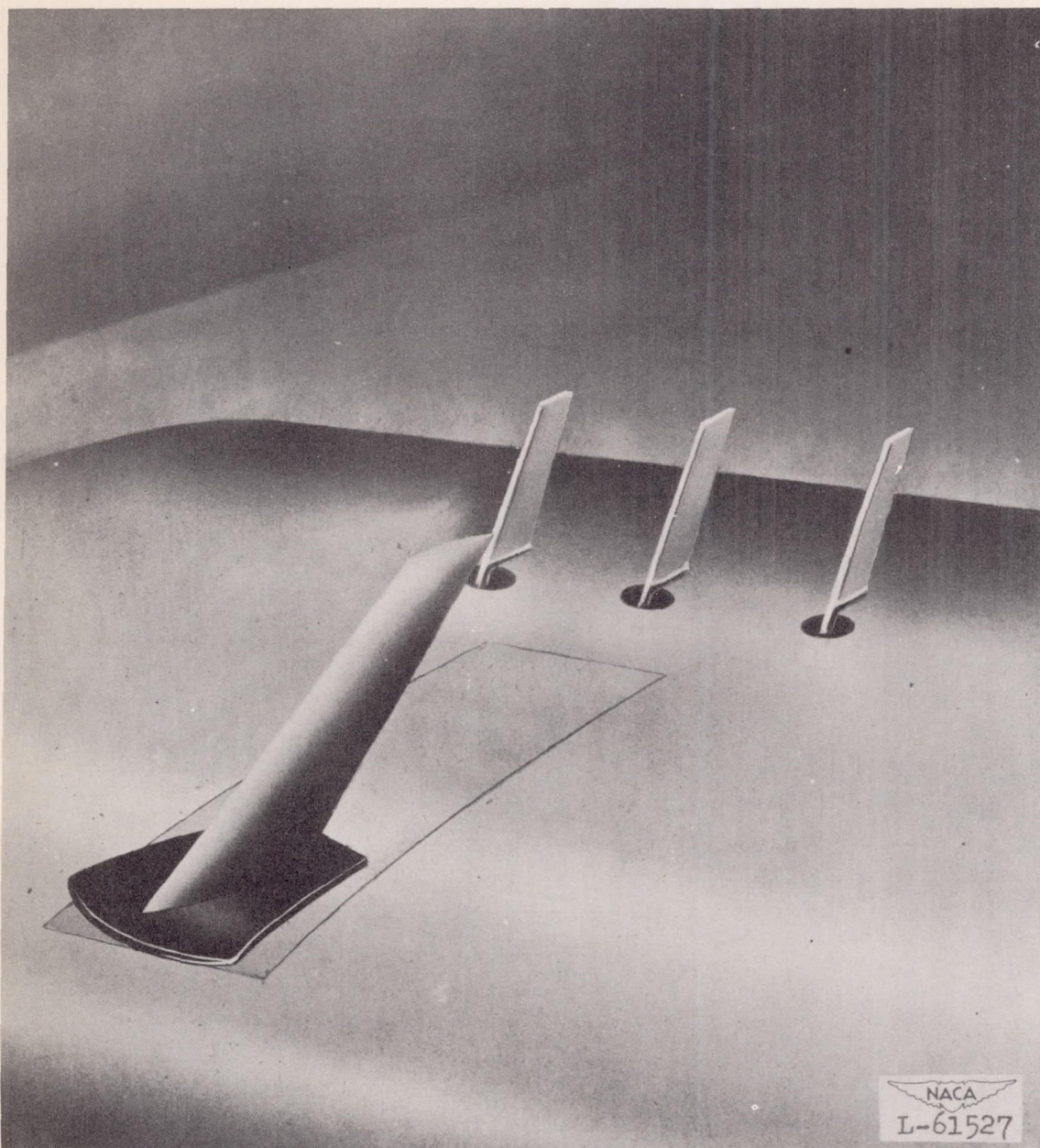
CONFIDENTIAL



(a) View showing model as tested.

Figure 4.- Model mounted on bump with three free-floating tails
installed.  Wing-alone configuration.
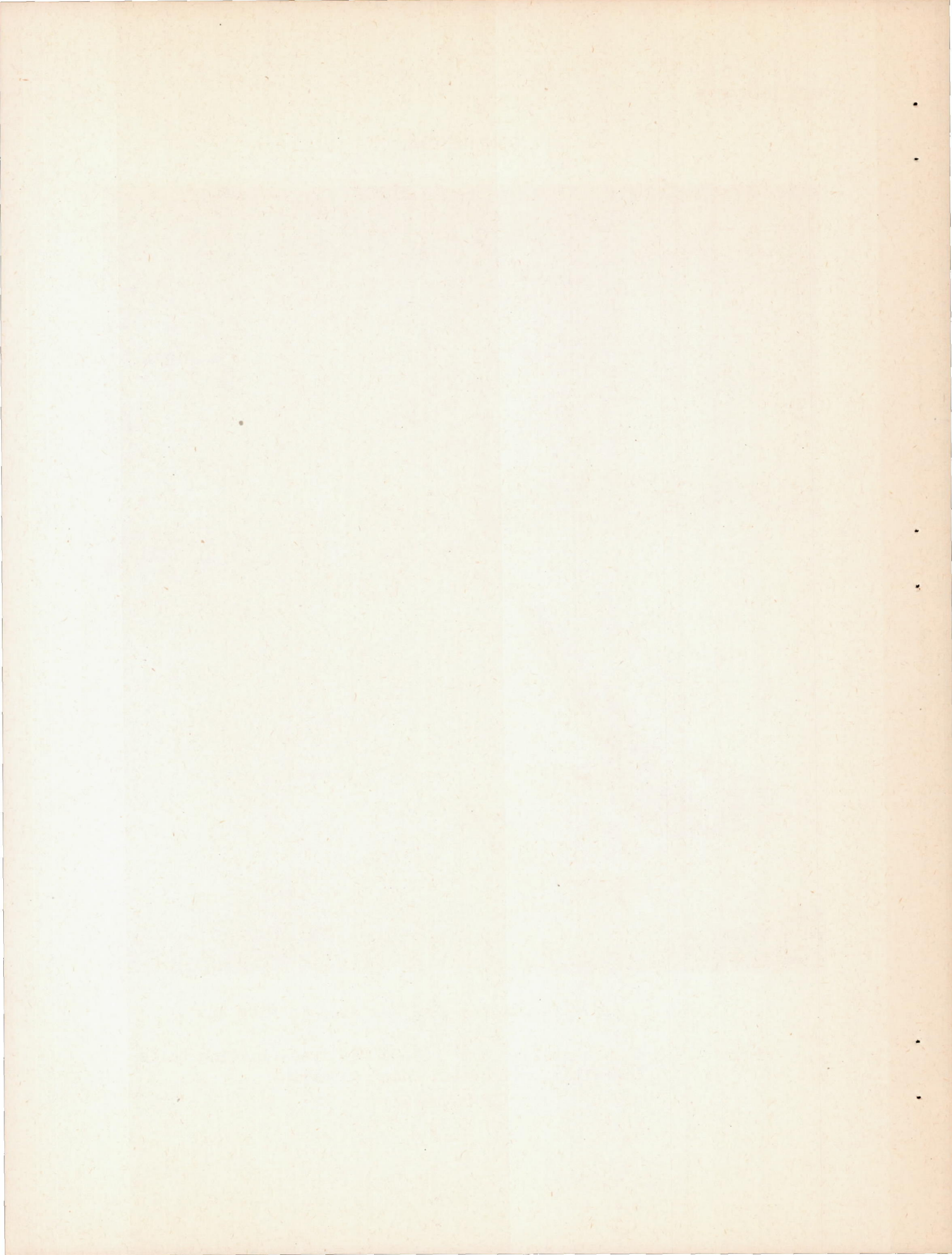
CONFIDENTIAL
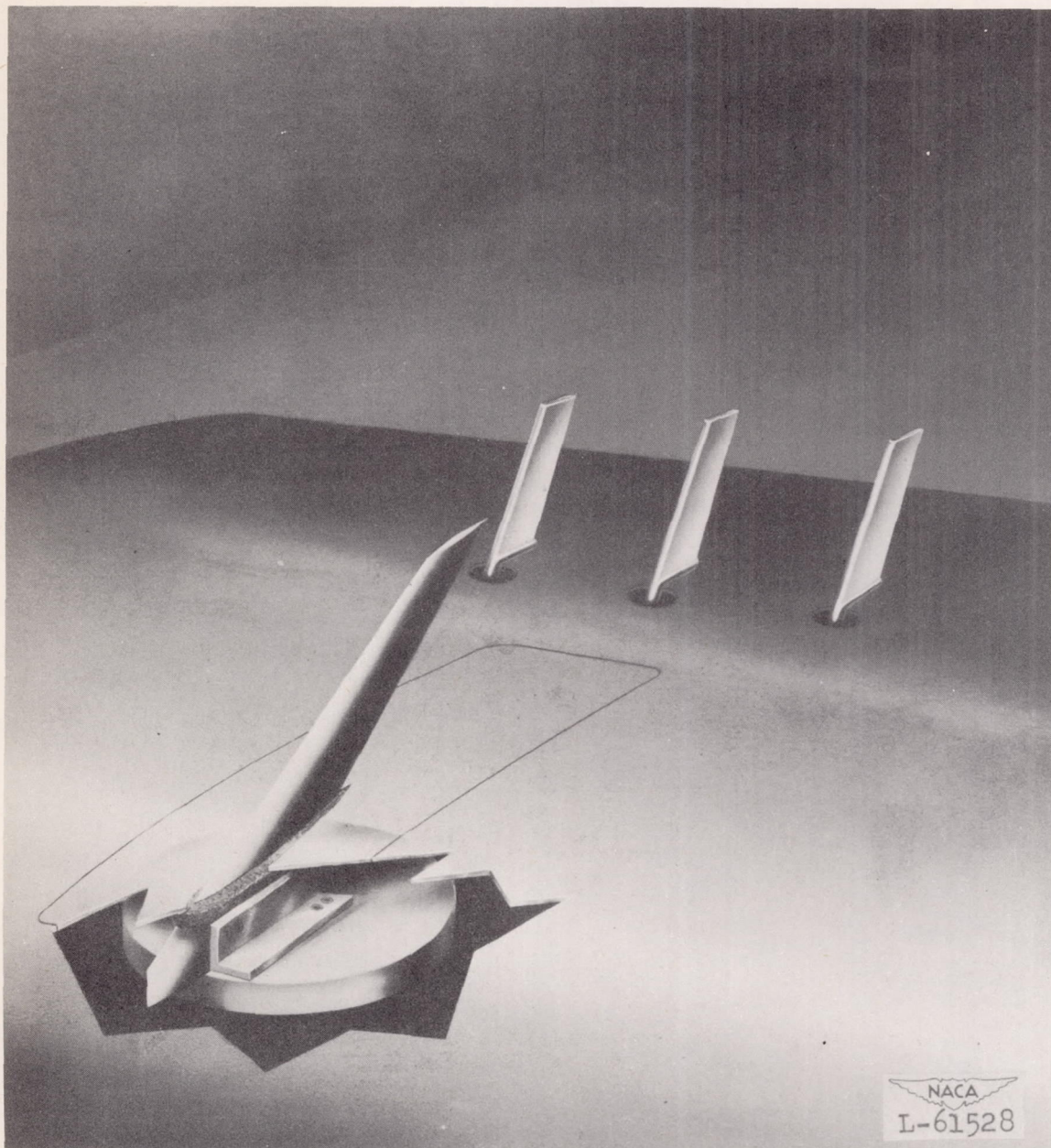
(b) Cutaway view showing seal fastened to wing butt.

Figure 4.- Concluded.

M=0.77      CONFIDENTIAL      M=0.90

M=1.00      M=1.17

——— —— ——— Nominal boundary-layer thickness

CONFIDENTIAL

Figure 5.- Typical Mach number contours over transonic bump in region of model location.
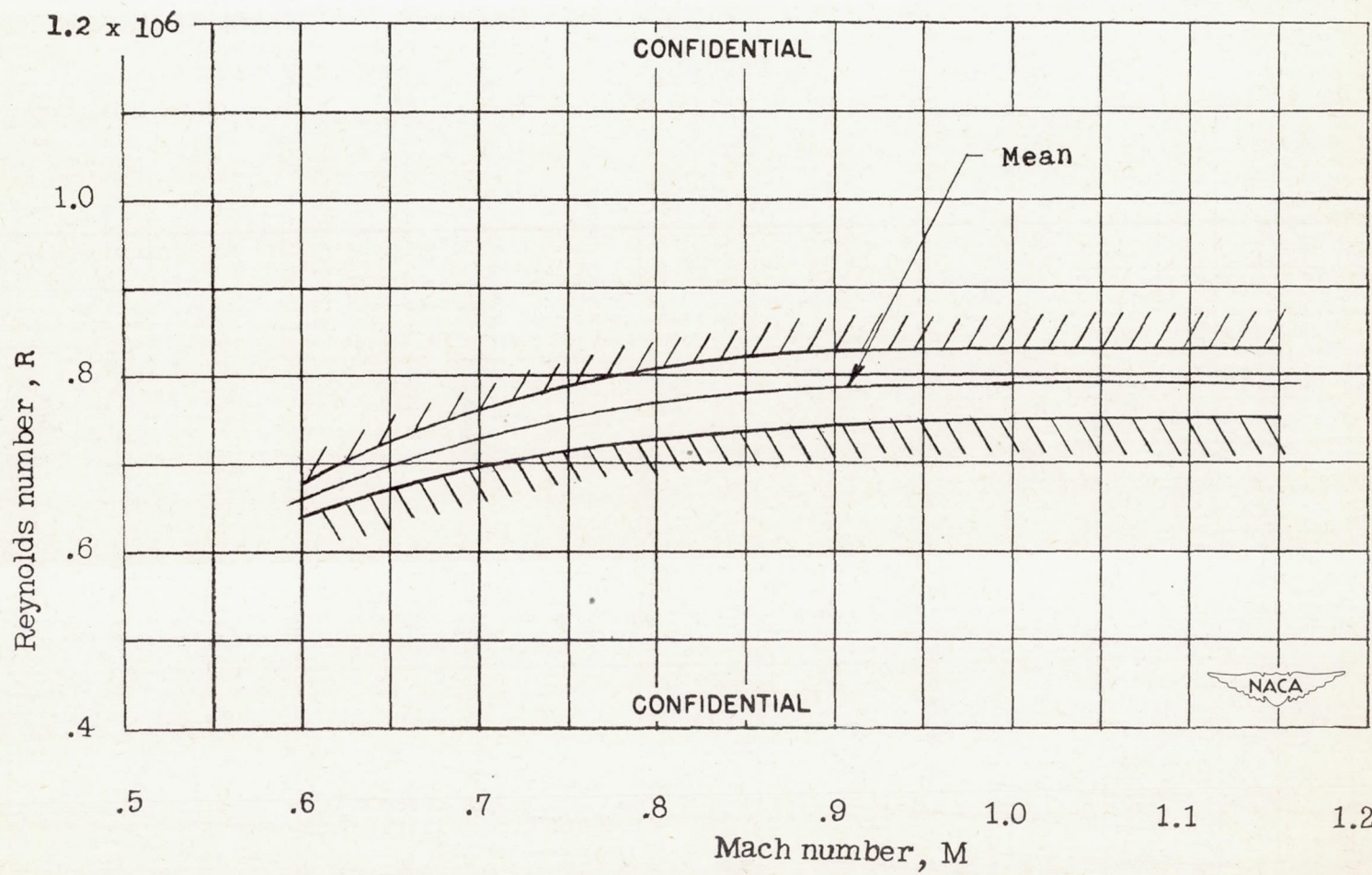
Figure 6.- Variation of test Reynolds number with Mach number for a model with 60° sweptback wing, aspect ratio 4, taper ratio 0.6, and NACA 65A006 airfoil.
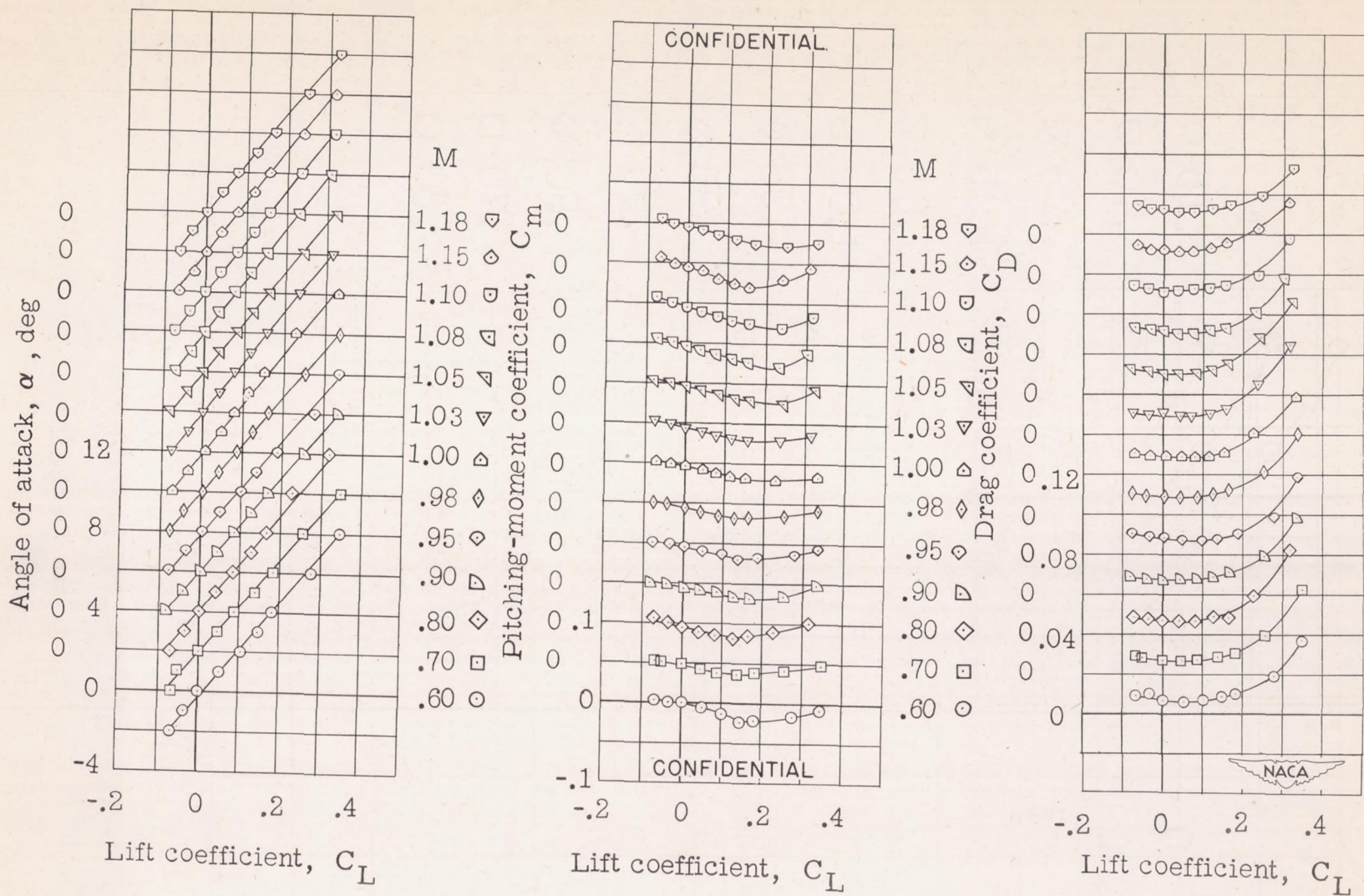
Figure 7.- Wing-alone aerodynamic characteristics for a model with 60° sweptback wing, aspect ratio 4, taper ratio 0.6, and NACA 65A006 airfoil.
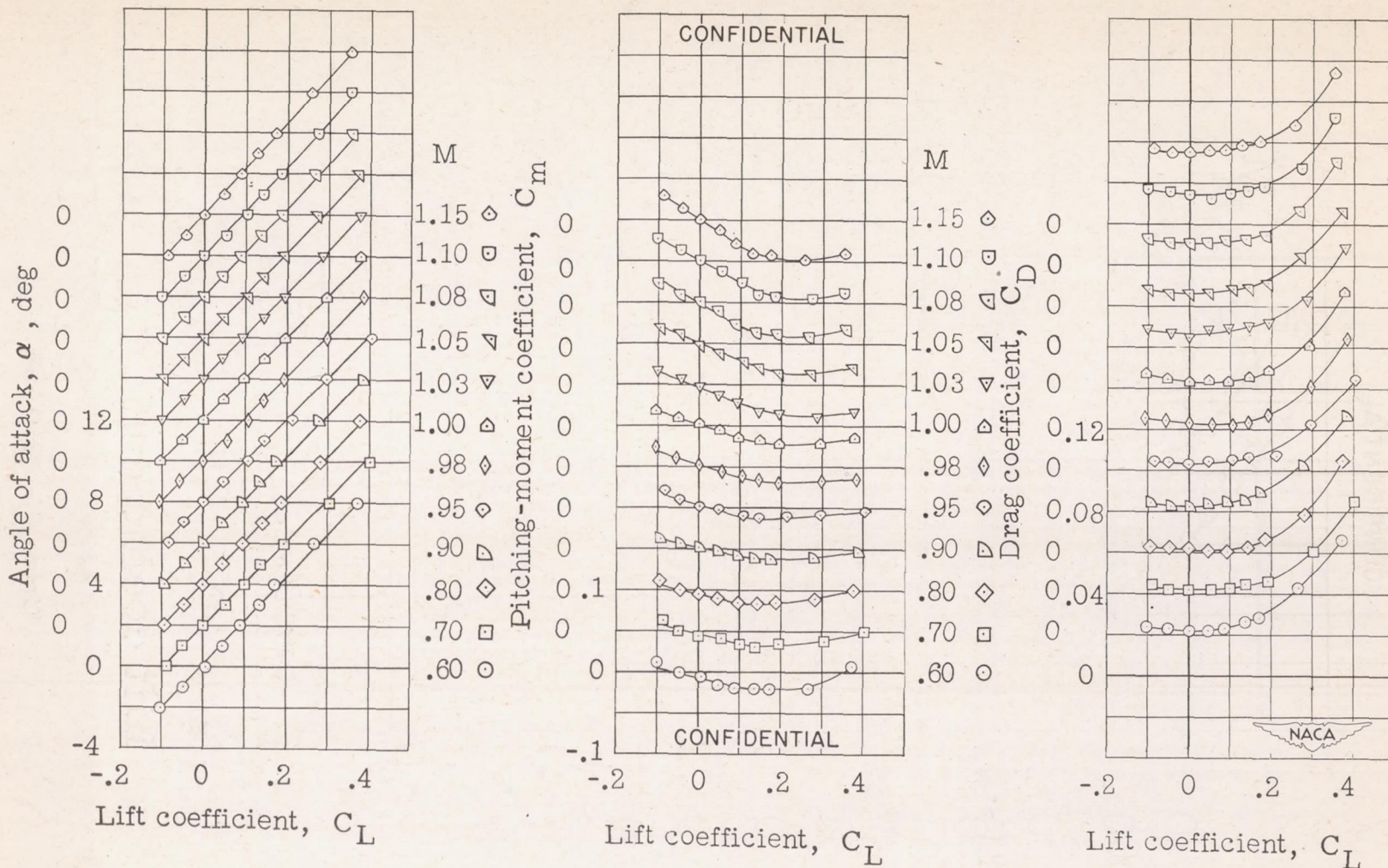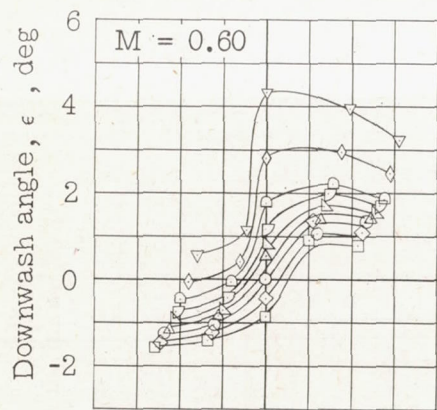
Figure 7.- Concluded.

Figure 8.- Wing-fuselage aerodynamic characteristics for a model with 60° sweptback wing, aspect ratio 4, taper ratio 0.6, and NACA 65A006 airfoil.
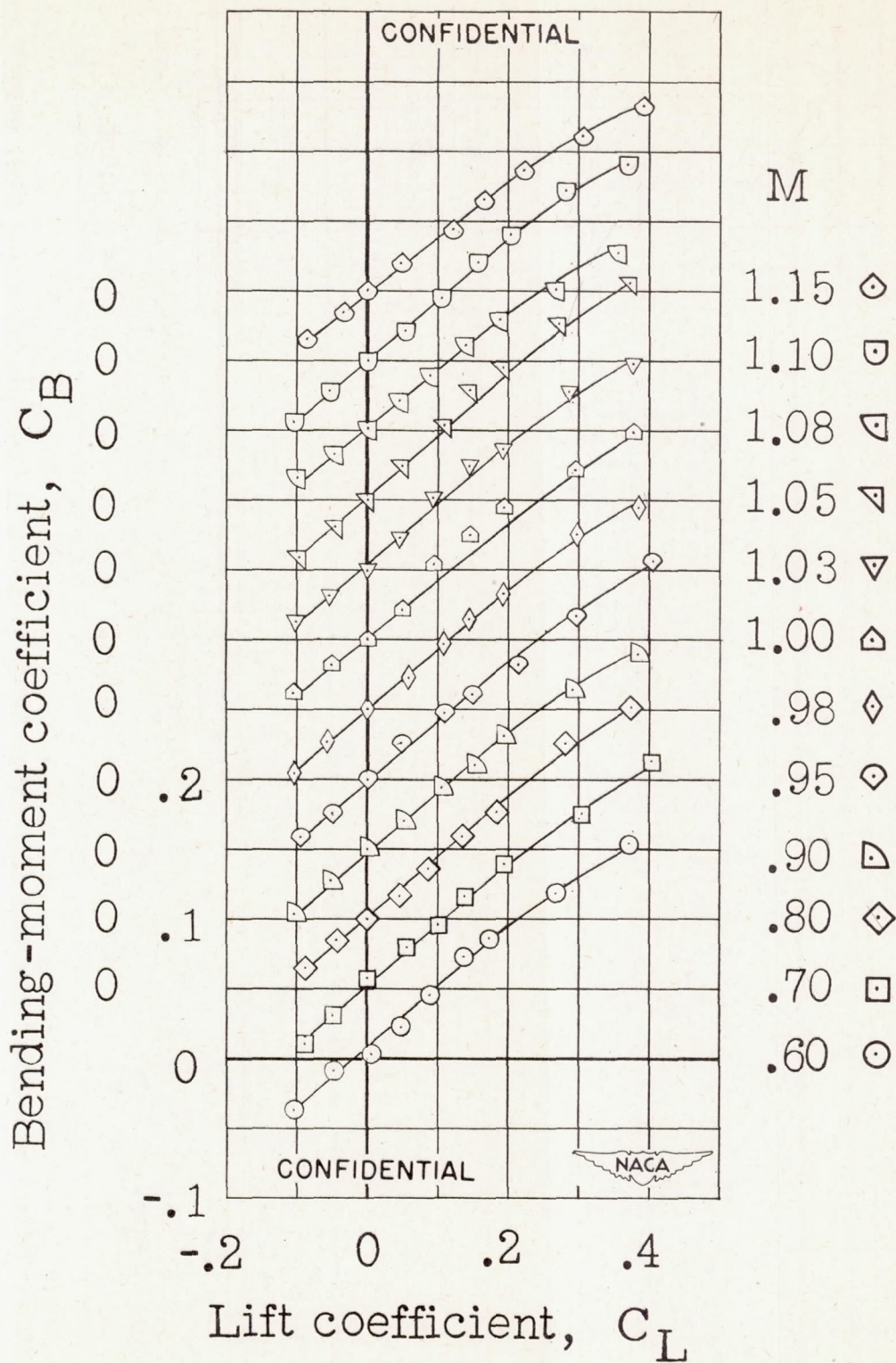
Figure 8.- Concluded.
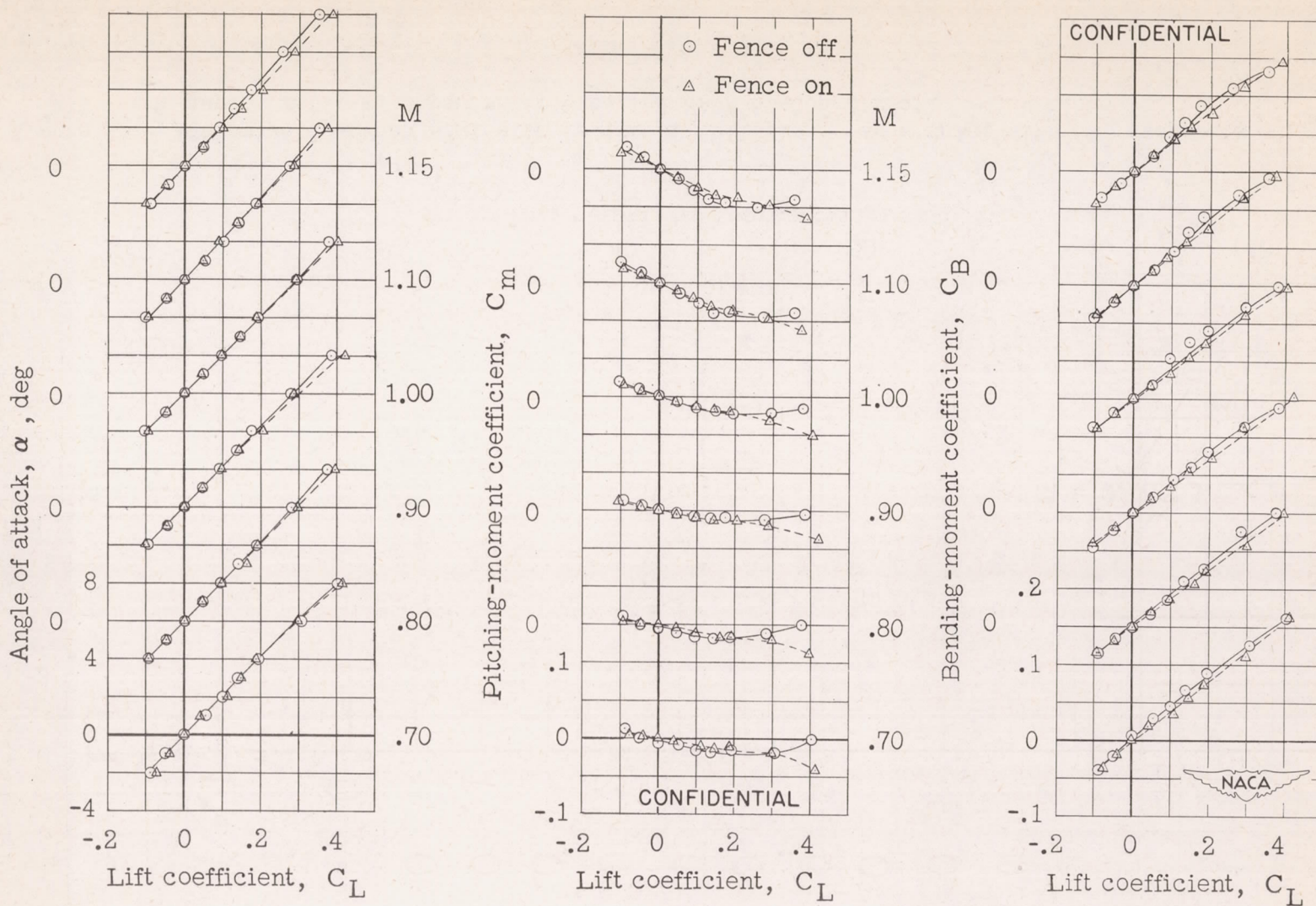
Figure 9.- Effect of wing fence on aerodynamic characteristics of a model with 60° sweptback wing, aspect ratio 4, taper ratio 0.6, and NACA 65A006 airfoil. Wing-fuselage.
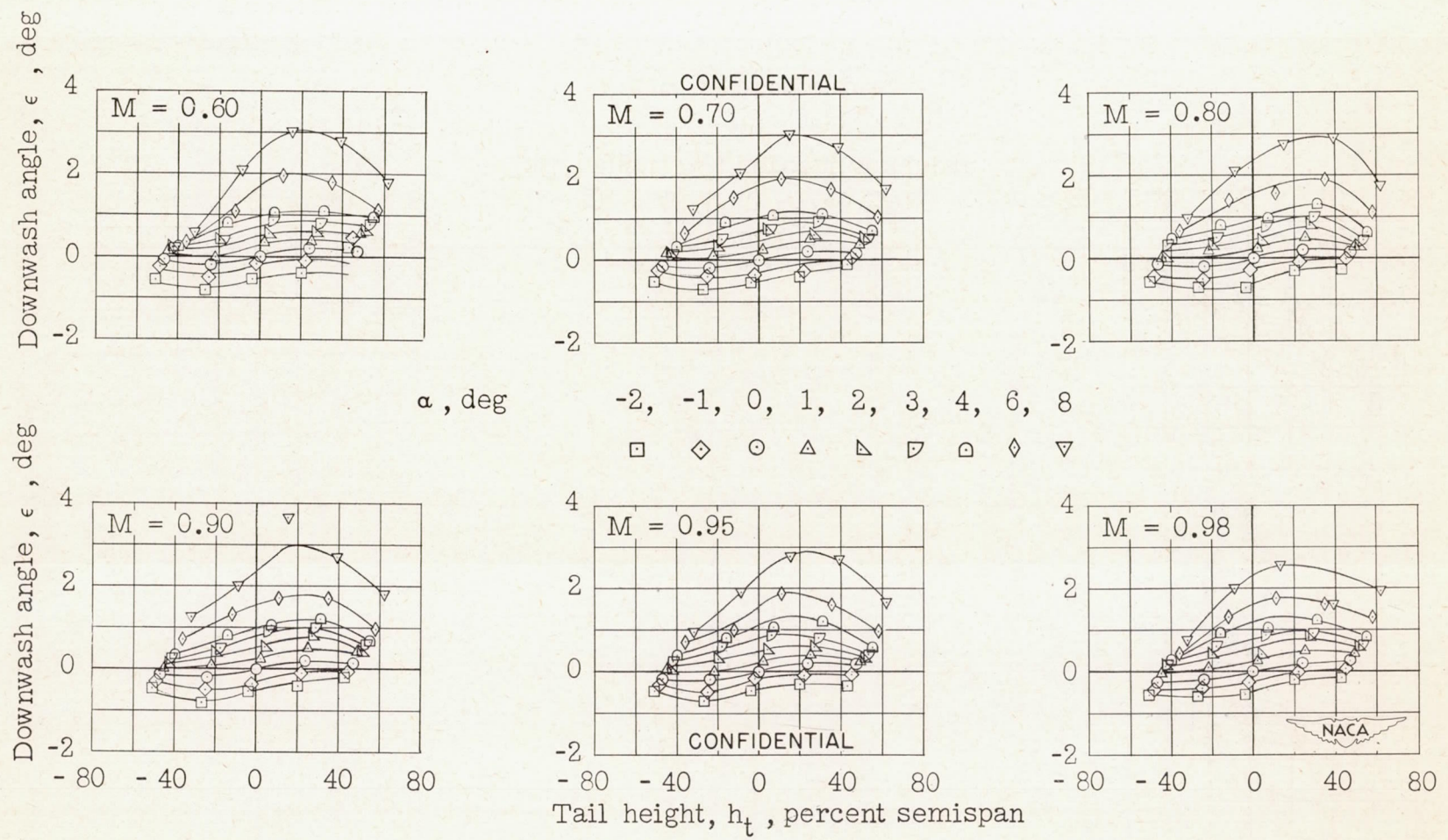
Figure 10.- Effective downwash angles in region of tail plane for a model with 60° sweptback wing, aspect ratio 4, taper ratio 0.6, and NACA 65A006 airfoil.  Wing alone.
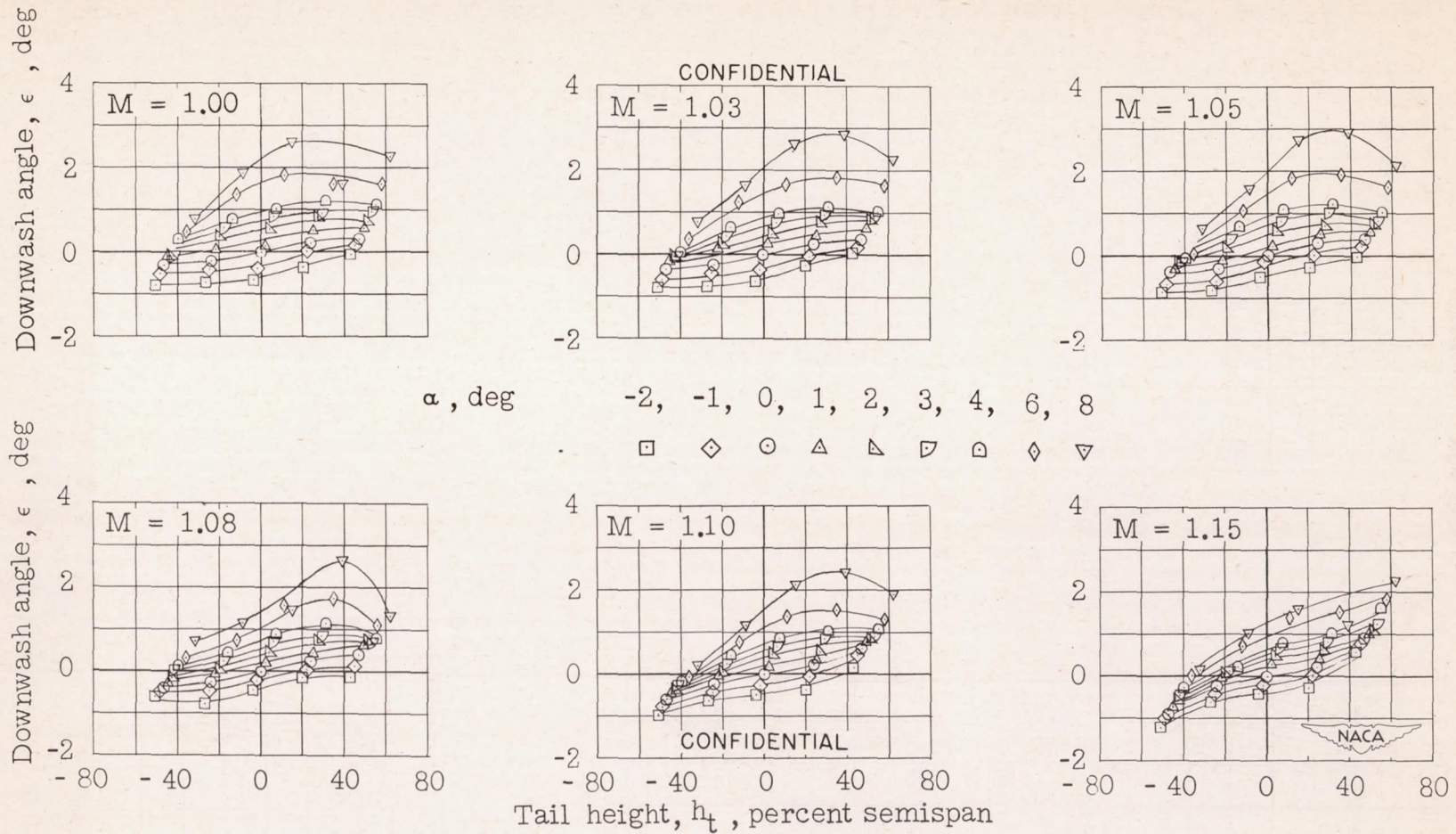
Figure 10.-Concluded.

CONFIDENTIAL

M = 0.60

M = 0.70

M = 0.80

$\alpha$ , deg        -2, -1, 0, 1, 2, 3, 4, 6, 8

M = 0.90

M = 0.95
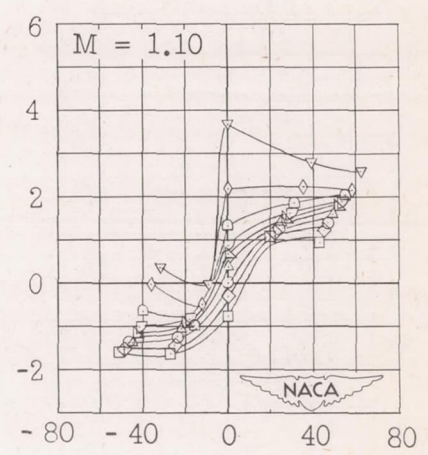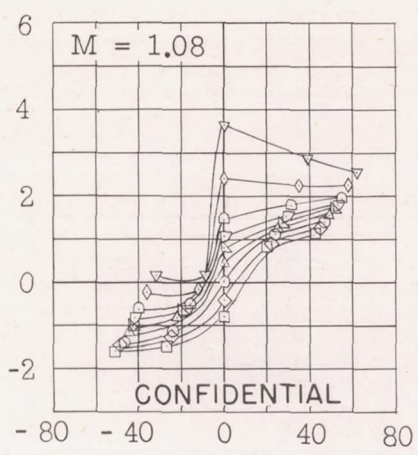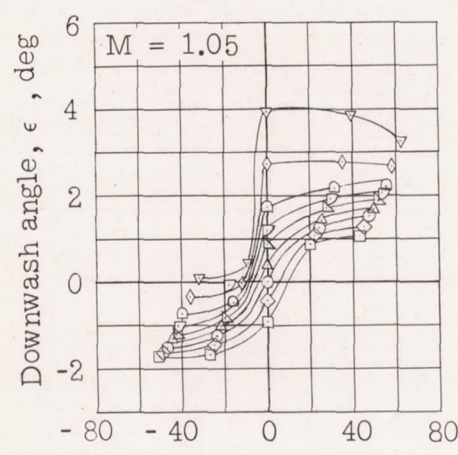
M = 0.98

CONFIDENTIAL
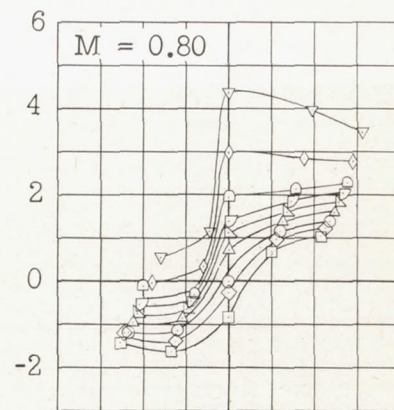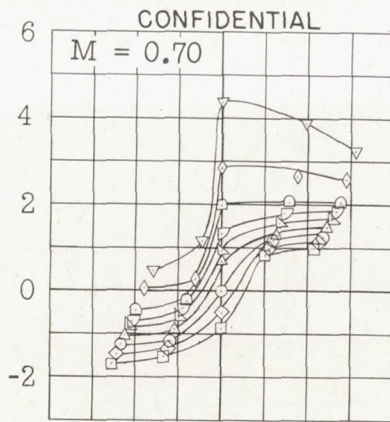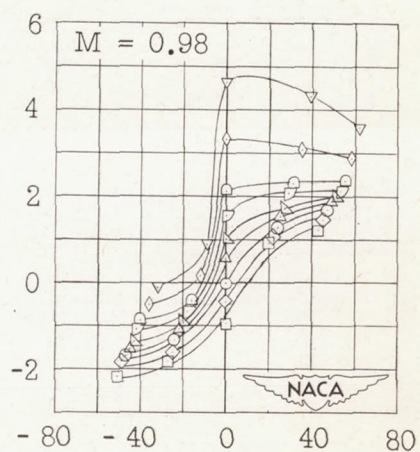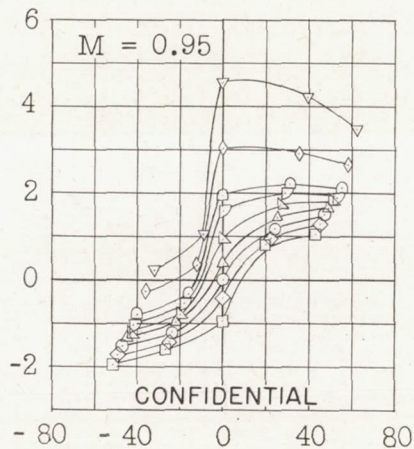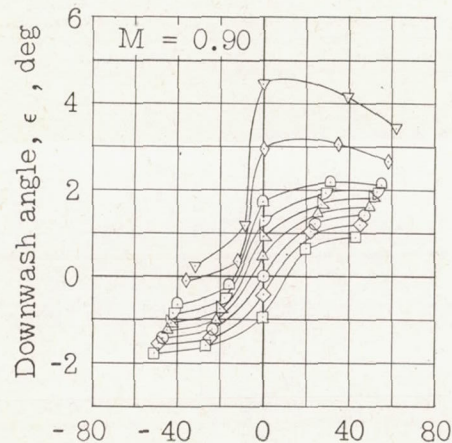
NACA

Tail height, $h_t$ , percent semispan

Figure 11.- Effective downwash angles in region of tail plane for a model with $60^\circ$ sweptback wing, aspect ratio 4, taper ratio 0.6, and NACA 65A006 airfoil. Wing-fuselage.
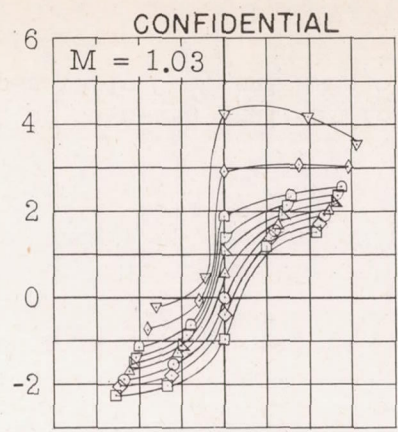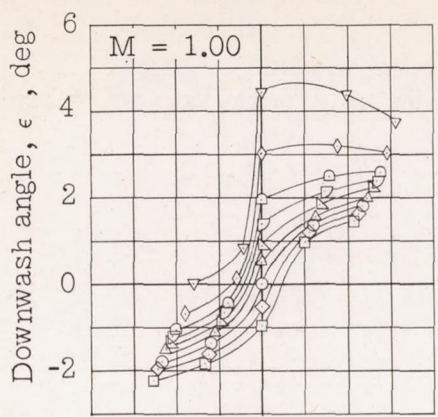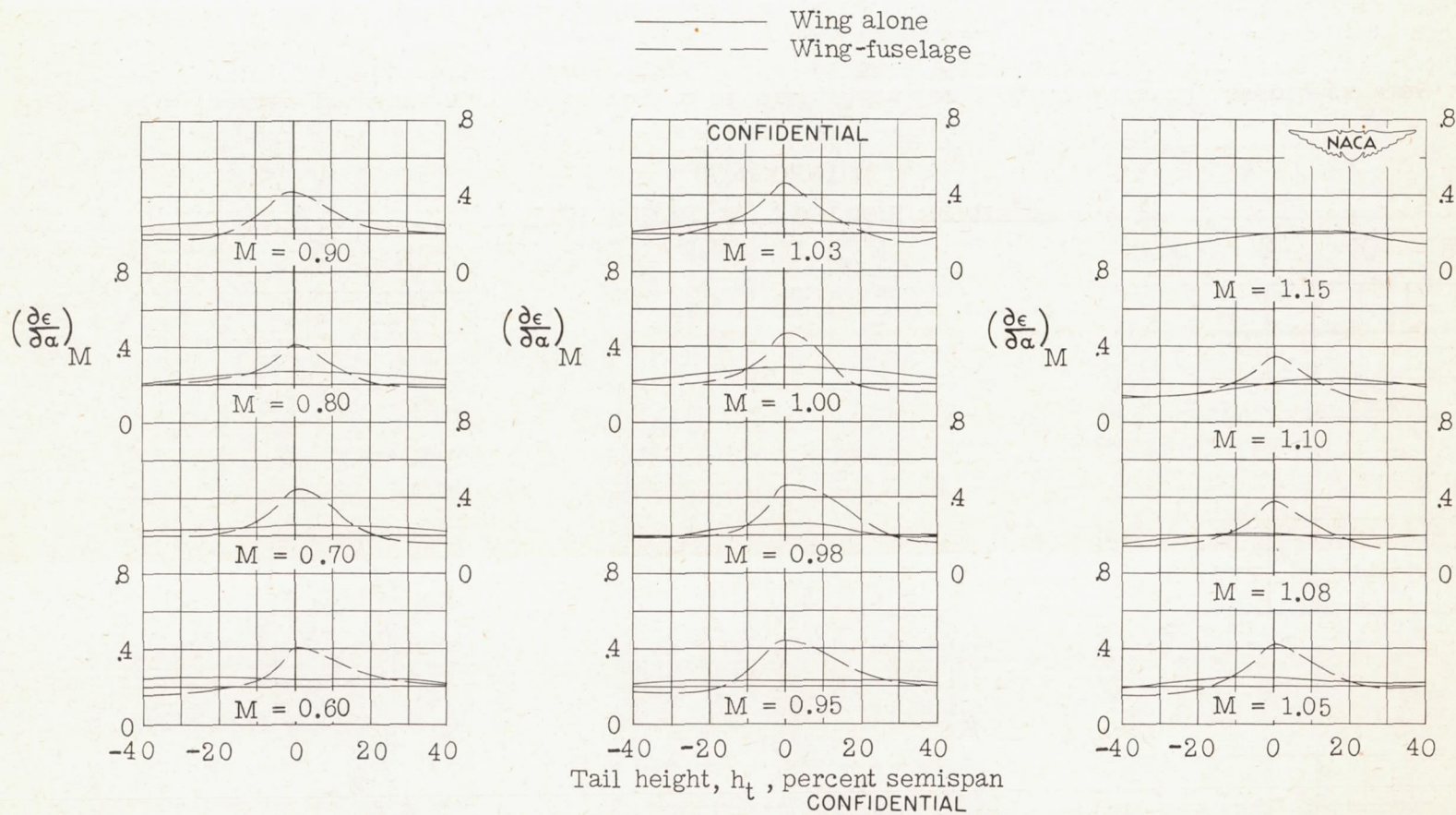
Figure 11.- Concluded.

Figure 12.- Variation with tail height of downwash gradient for a model with 60° sweptback wing, aspect ratio 4, taper ratio 0.6, and NACA 65A006 airfoil.

CONFIDENTIAL

$M = 0.60$          $\alpha = 7^0$          $M = 0.70$          $\alpha = 7^0$          $M = 0.80$

—————— Wing alone
− − − − − − Wing -fuselage

$\alpha = 4^0$          $\alpha = 4^0$

$\alpha = 0^0$          $\alpha = 0^0$

− 80   − 40   0   40   80   − 80   − 40   0   40   80   − 80   − 40   0   40   80

Tail height, $h_t$ , percent semispan
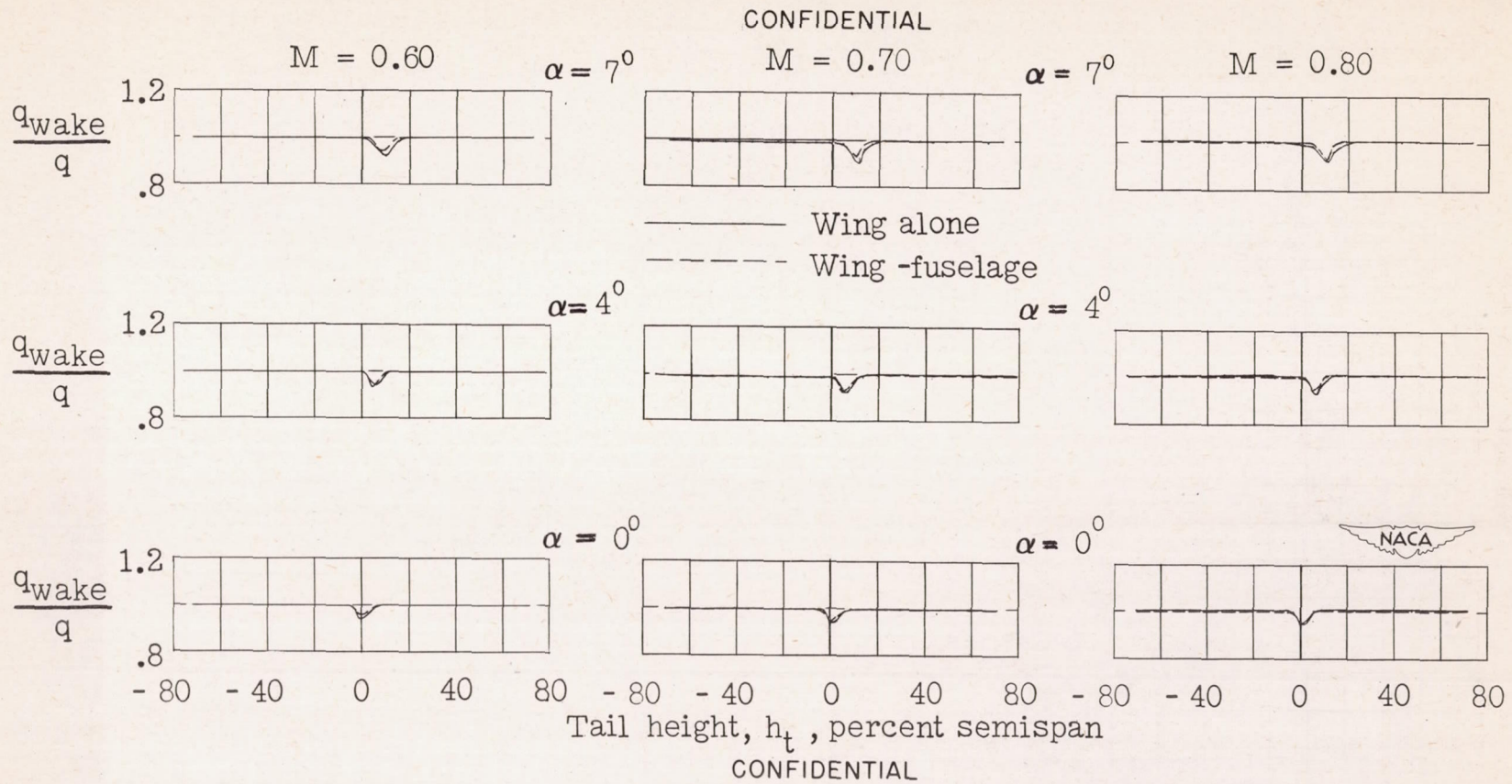
CONFIDENTIAL

Figure 13.- Dynamic-pressure surveys in region of tail plane for a model with 60° sweptback wing, aspect ratio 4, taper ratio 0.6, and NACA 65A006 airfoil.

CONFIDENTIAL

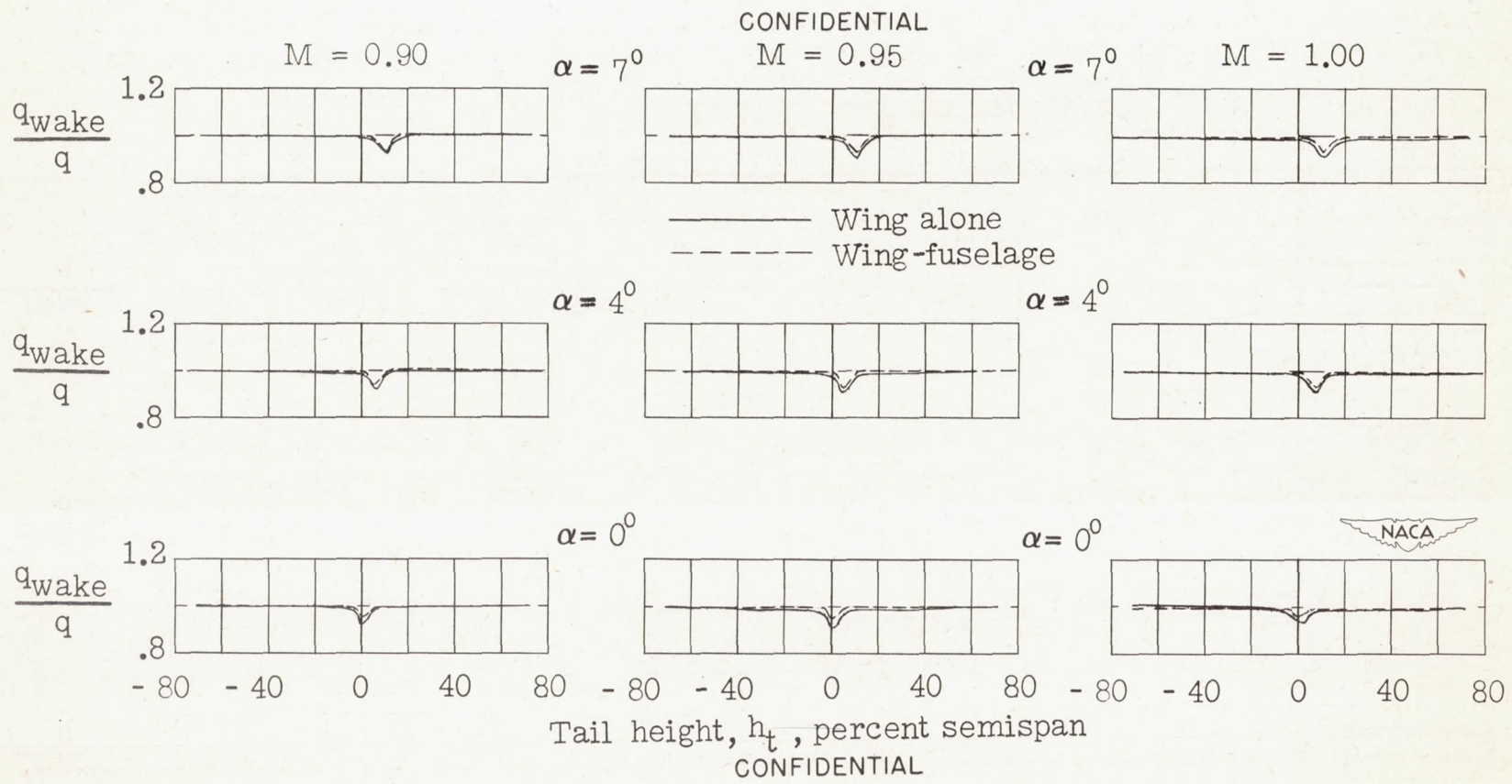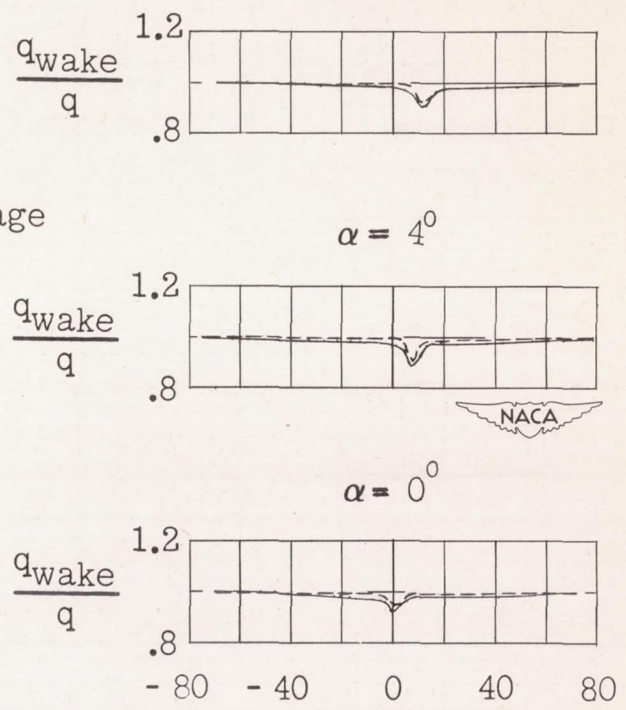M = 0.90     $\alpha = 7^0$     M = 0.95     $\alpha = 7^0$     M = 1.00

———— Wing alone
— — — — Wing-fuselage

$\alpha = 4^0$     $\alpha = 4^0$

$\alpha = 0^0$     $\alpha = 0^0$

Tail height, $h_t$ , percent semispan
CONFIDENTIAL

Figure 13.- Continued.

M = 1.05

M = 1.10

$\alpha = 7^0$

$\alpha = 7^0$

$\frac{q_{wake}}{q}$

$\frac{q_{wake}}{q}$

————— Wing alone
— — — — Wing-fuselage

$\alpha = 4^0$

$\alpha = 4^0$

$\frac{q_{wake}}{q}$

$\frac{q_{wake}}{q}$

$\alpha = 0^0$

$\alpha = 0^0$

$\frac{q_{wake}}{q}$

$\frac{q_{wake}}{q}$

-80    -40    0    40    80

-80    -40    0    40    80

Tail height, $h_t$ , percent semispan

Figure 13.- Concluded.
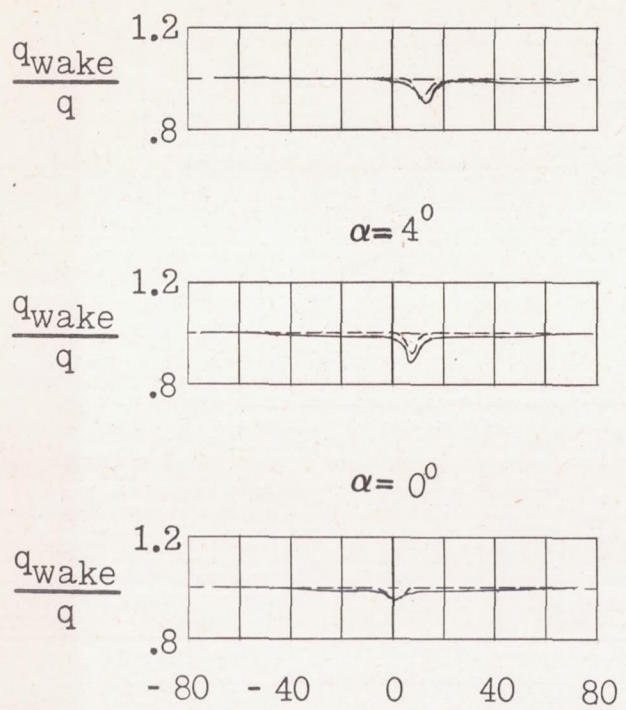
———— Wing alone
– – – – Wing-fuselage

CONFIDENTIAL

$C_{D_{L=0}}$    .04    0

$\left(\dfrac{\partial \epsilon}{\partial \alpha}\right)_M$    .8    .4    0

$h_t$    0    30    -30    0    30    -30

$\left(\dfrac{\partial C_L}{\partial \alpha}\right)_M$    .08    .04    0

$\left(\dfrac{\partial \epsilon}{\partial \alpha}\right)_M$    .8    4    0

$h_t$    0    -30    30    -30    30

$\left(\dfrac{\partial C_m}{\partial C_L}\right)_M$    0    -.2    -.4

.6    .7    .8    .9    1.0    1.1    1.2
Mach number, M

$\dfrac{q_{wake}}{q}$    1.2    .8

$h_t$    ±30    NACA    0

CONFIDENTIAL

.6    .7    .8    .9    1.0    1.1    1.2
Mach number, M

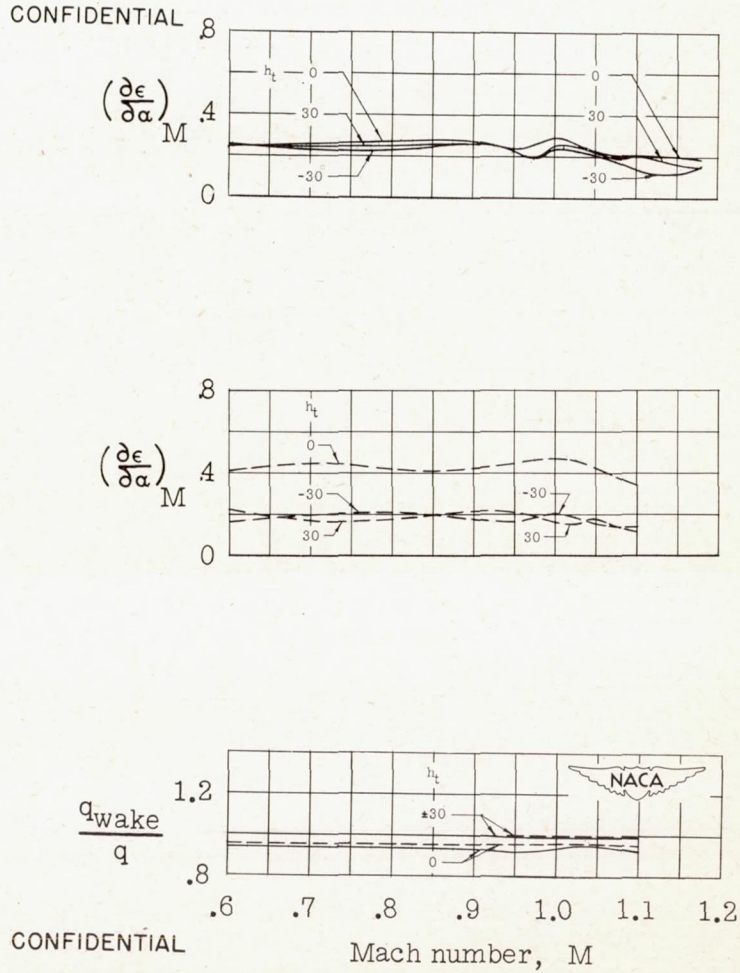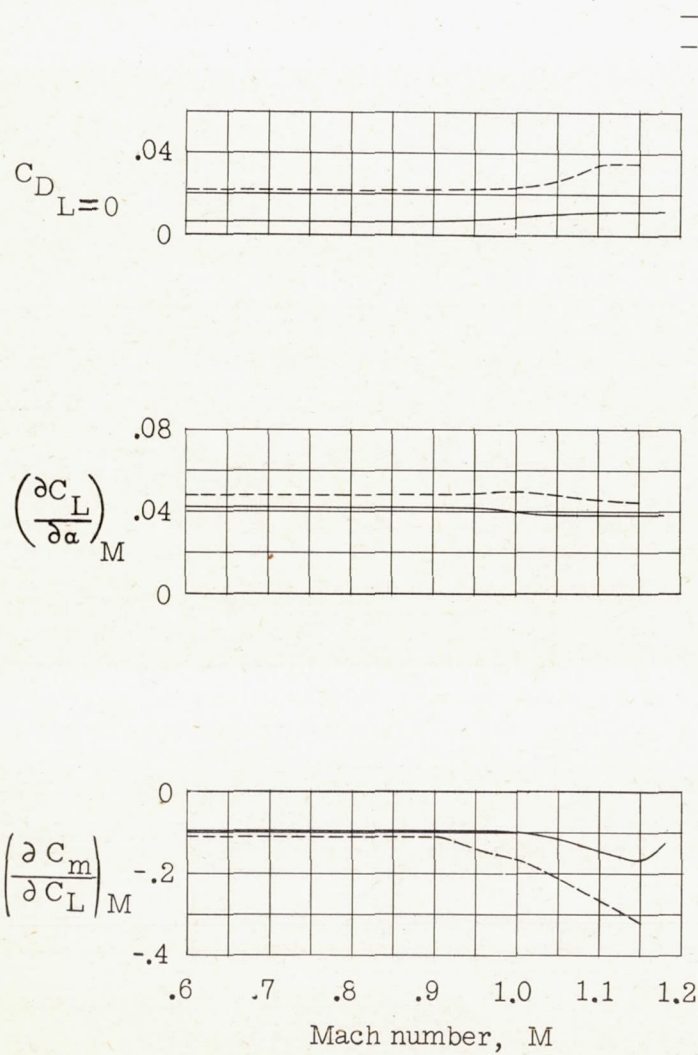Figure 14.- Summary of aerodynamic characteristics for a model with 60° sweptback wing, aspect ratio 4, taper ratio 0.6, and NACA 65A006 airfoil. $C_L = 0$.